Available online at www.sciencedirect.com
SCIENCE DIRECT®
Tetrahedron xx (2006) 1–7
Tetrahedron

Stilbene like carbazole dimer-based electroluminescent materials

Chih-Hsin Chen,[a,b] Jiann T. Lin[a,*] and Ming-Chang P. Yeh[b,*]

[a]*Institute of Chemistry, Academia Sinica, 128 Sec. 2, Academia Rd, Nankang, Taipei 115, Taiwan*
[b]*Department of Chemistry, National Taiwan Normal University, 88 Sec. 4, Ting-Chow Rd, Taipei 116, Taiwan*

Received 9 May 2006; revised 13 June 2006; accepted 19 June 2006

Abstract—Two carbazole dimers (**1** and **10**) were synthesized from 9-ethyl-9*H*-carbazole-3-carbaldehyde and 6-bromo-9-ethyl-9*H*-carbazole-3-carbaldehyde by McMurry C–C coupling reaction. Palladium(0)-catalyzed C–N coupling reactions of **10** and various diarylamines result in the formation of stable carbazole derivatives in good yields. These compounds are fluorescent in blue to yellow region with moderate to good quantum yields. Also, they are thermally stable and capable of hole-transporting due to the presence of the carbazole moieties. The electroluminescent devices fabricated using **1**, **2**, and **3** as hole-transporters/emitters with a bilayer structure ITO/**Cpd**/TPBI or Alq_3/LiF/Al (**Cpd**=**1**, **2**, and **3**) exhibit good performance (e.g., η_{ext}=1.0–2.1%; η_p=0.9–1.9 lm/W; η_c=2.4–4.8 cd/A at a current density of 100 mA/cm^2).
© 2006 Elsevier Ltd. All rights reserved.

1. Introduction

Considerable progress has been made on organic light emitting diodes (OLEDs) since the seminal report by Tang et al., on the device with a double-layer structure.[1] Now OLEDs have become visible in consumer electronics such as car stereos, mobile phones, and digital cameras. Appropriate choosing of the electron- and hole-transporting materials is necessary in order to have high performance small molecules[2] or polymeric[3] OLEDs. The durability of the devices, which depends on the thermal and morphological stability of the organic films, is also a key factor in affecting the device performances. We have been interested in the development of new materials for OLED application. We found that carbazolyl unit is beneficial to raise both glass transition temperature and thermal stability of luminescent chromophores.[4] Further, it is relatively easy to functionalize the carbazolyl moiety at the 3-, 6-, or 9-positions for tuning its physical properties. A variety of carbazole derivatives, including small molecules,[4] dendrimers,[5] or polymers,[6] which served as hosts,[7] dopants,[8] hole-transporters,[9] or emitters with a wide color range,[10] have been reported. Recent developments in carbazole derivatives and their application as advanced amorphous materials for photorefractive systems, organic light emitting diodes as well as other optoelectronic devices are investigated.[11] Earlier we synthesized a series of compounds containing a carbazolyl core encapsulated with peripheral arylamines. These materials were found to be green or blue emitting and capable of hole-transporting.[4] In this report, we further integrated two carbazole moieties by McMurry C–C coupling reaction. For the sake of tuning the emission color in visible light region or altering energy level to adjust the ability of hole injection, the stilbene like carbazole dimer was followed by encapsulation with arylamines. Although, the stilbene-containing materials[11,12] and oligomeric carbazolyl compounds[13] were reported for electroluminescent applications, to our knowledge, no stilbene like carbazole dimer-based electroluminescent materials have been reported so far. Double-layer EL devices using these compounds as hole-transporting layer and emitting layer and Alq_3 [tris(8-quinolinolato)aluminum][14] or TPBI [1,3,5-tris(*N*-phenyl-benzimidazol-2-yl)benzene][15] as electron-transporting layer were fabricated by vacuum deposition.

2. Results and discussion

The compounds for electroluminescent study are depicted in Figure 1. Scheme 1 illustrates the synthesis of these new compounds. 9-Ethyl-9*H*-carbazole-3-carbaldehyde (**8**) was obtained starting from ethylation of carbazole followed by treating the resulting 9-ethyl-9*H*-carbazole with $POCl_3$ in DMF via Vilsmeier–Haack reaction[16] in 65% yield. Compound **8** was further treated with NBS (*N*-bromosuccinimide) to give 6-bromo-9-ethyl-9*H*-carbazole-3-carbaldehyde (**9**), which reacted with titanium(IV) chloride and zinc powder to afford **10** in good yield (85%). Finally, palladium-catalyzed coupling reactions[17] of **10** with arylamines using $Pd(OAc)_2$/P(*t*-Bu)$_3$ as the catalyst and *t*-BuONa as the base resulted in efficient C–N bond formation to give

Keywords: Carbazole dimmer; Electroluminescent; McMurry C–C coupling reaction.
* Corresponding authors. Tel.: +886 2 27898522; fax: +886 2 27831237 (J.-T.L.); tel.: +886 2 29320204; fax: +886 2 29341742 (M.-C.P.Y.); e-mail addresses: jtlin@chem.sinica.edu.tw; cheyeh@scc.ntnu.edu.tw

0040–4020/$ - see front matter © 2006 Elsevier Ltd. All rights reserved.
doi:10.1016/j.tet.2006.06.067

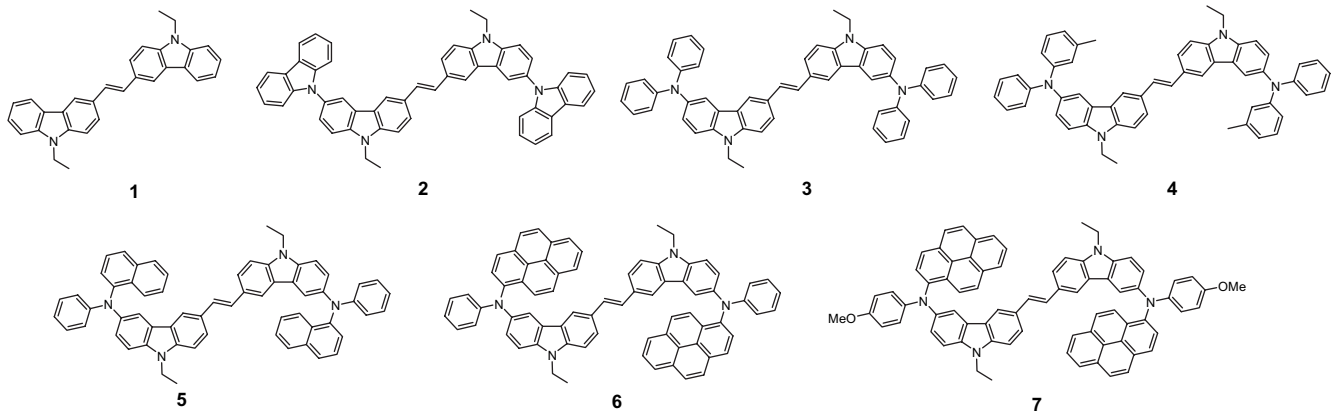

Figure 1. Structure of the compounds.

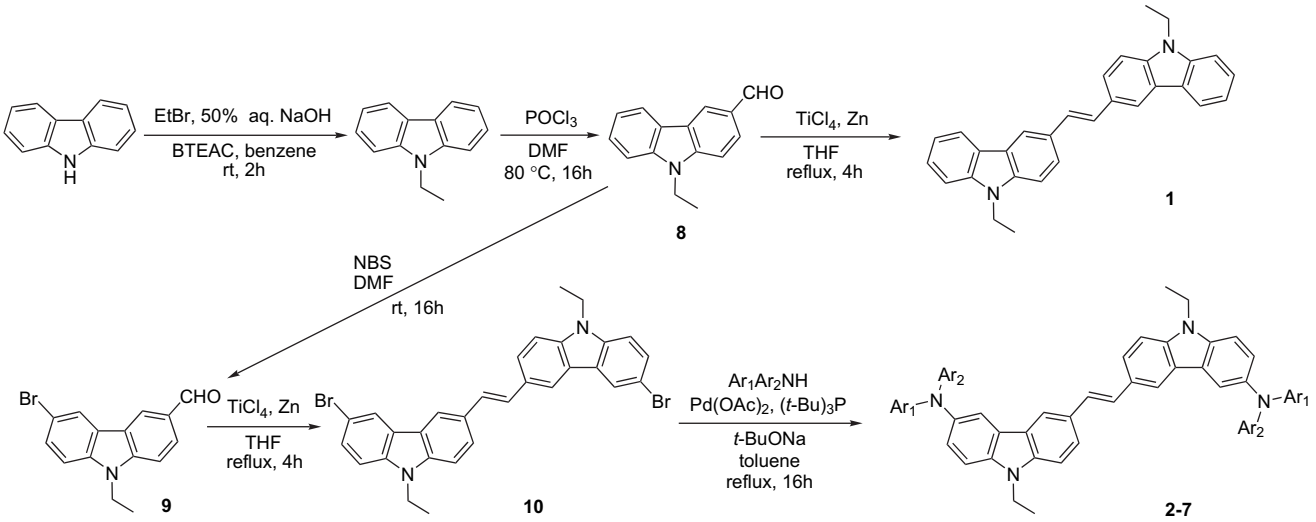

Scheme 1.

diaminocarbazole dimers **2**–**7**. It must be mentioned that the reactions readily occurred at lower temperature (ca. 80 °C) to form both *Z*- and *E*-isomers. However, higher reaction temperature (reflux in toluene) gave predominantly *E*-form in 65 to 80% yields. All the target products were soluble in common organic solvents such as CH_2Cl_2, $CHCl_3$, or THF so that all these diaminocarbazole dimers can be easily purified by flash column chromatography. Compounds **1**–**7** were fully characterized by ^1H and ^{13}C NMR spectroscopies, mass spectroscopy, and elementary analyses. The thermal properties of the compounds were determined by DSC (differential scanning calorimetry) and TGA (thermogravimetric analysis) measurements (Table 1). All the compounds except **5** and **7** are crystalline. No crystallization and

Table 1. Physical properties of the compounds

Compd	λ_{abs},[a] nm	λ_{em},[a] nm (Φ_f,[b] %)	λ_{em},[c] nm (Φ_f,[b] %)	λ_{em},[d] nm	T_m/T_d,[e] °C	E_{ox} (ΔE_p),[f] mV	HOMO, eV	LUMO, eV
1	308, 342	411 (40)	407 (44)	447	218/268	245 (92), 555 (82)	5.05	2.05
2	294, 344	416 (45)	412 (49)	451	335/403	370 (55), 676 (i)	5.17	2.17
3	309, 346	434 (18)	422 (10)	463	284/349	201 (120), 755 (i)	5.00	2.05
4	310, 347	441 (20)	421 (8)	468	207/370	190 (68), 764 (i)	4.99	2.04
5	306, 344	507 (9)	454 (8)	472	na/382	198 (142), 769 (i)	5.00	2.07
6	321, 356	549 (16)	503 (33)	523	295/403	192 (144), 690 (i)	4.99	2.33
7	334, 361	560 (20)	516 (35)	545	na/468	107 (114), 601 (i)	4.91	2.34

Oxidation potential reported is adjusted to the potential of ferrocene ($E_{1/2}$=245 mV vs $Ag/AgNO_3$), which was used as an internal reference. Conditions of cyclic voltammetric measurements: glassy carbon working electrode; $Ag/AgNO_3$ reference electrode. Scan rate: 100 mV/s. Electrolyte: tetrabutylammonium hexafluorophosphate; i, irreversible process. HOMO calculated from CV potentials using ferrocene as standard [HOMO=4.8+($E_{ox}-E_{Fc}$)]. LUMO derived from the relationship E_g) HOMO−LUMO, where E_g was obtained from optical spectroscopy; na: not available.

[a] Recorded in dichloromethane solutions.

[b] Quantum yield was measured with reference to Coumarin 1 (99%) in ethyl acetate. Refractive index change due to the use of different solvent correction was applied in the calculation.

[c] Recorded in toluene solutions.

[d] Film samples.

[e] Decomposition temperature (T_d) corresponds to the 5% weight loss.

[f] Recorded in dichloromethane solutions.

melting were noticed for these compounds after fast cooling of the melt. However, no glass transition can be detected. The thermal decomposition temperatures of these compounds range from 268 to 468 °C. Introduction of arylamines into the central carbazole dimer greatly enhanced the decomposition temperature (T_d) of the materials. This effect is prominent when the carbazole (**2**) or pyrenyl amine (**6** and **7**) is introduced at 3- and 3′-positions.

The photophysical properties of the carbazole dimer derivatives were examined by UV–vis and fluorescence spectroscopies in both dichloromethane and toluene solutions. The absorption and emission spectra of the compounds in dichloromethane were shown in Figure 2. In general, each of these compounds has absorption at ~350 nm, which was assigned to π–π* transition of the carbazole dimer core. In addition, there exist localized π–π* transition due to end-capping arylamines such as carbazole, diphenylamine, *N*-phenylnaphthalen-1-amine, or *N*-phenylpyren-1-amine. Compounds **6** and **7**, which have pyrene moieties display an extra band at the longer wavelength due to pyrenyl amine. These compounds emit blue to yellow light with emission maxima ranging from 416 to 560 nm in dichloromethane solution. The emission of **2** is almost identical to the emission of the central carbazole dimer (compound **1**), possibly due to the weak donating ability of the carbazolyl moiety and the noncoplanarity between the carbazolyl moiety and central core. All other compounds, **3**–**7**, have better conjugation between the periphery arylamines and the central core, and exhibit longer λ_{em}. No solvatochromic effect in the absorption spectra was observed. However, there is significant dipolar character in the excited state of the compounds **5**–**7** in view of the large positive solvatochromic effect in more polar solvent ($\lambda_{em}(CH_2Cl_2)-\lambda_{em}$(toluene)>45 nm).

From cyclic voltammetric measurements and square wave voltammetric methods, the electrochemical properties of the compounds were studied and the redox potentials of the compounds are compiled in Table 1. Compound **1** exhibits two reversible one-electron redox waves, which indicates that there exist some electronic communications between the two carbazole moieties and cause them to be oxidized individually.[18] In addition, compounds **2**–**7**, in which the carbazole dimer was incorporated with arylamines, exhibit two reversible one-electron redox waves, which are barely resolvable and an irreversible two-electron wave due to the oxidation of the peripheral diarylamines and the central carbazole dimer (Table 1 and Fig. 3), respectively. The first oxidation potential decreases (**2**>**3**>**5**>**4**>**6**>**7**) in accordance with the electron donating ability of the substituent at the nitrogen atoms of the peripheral amines. Lack of electronic communication between the two

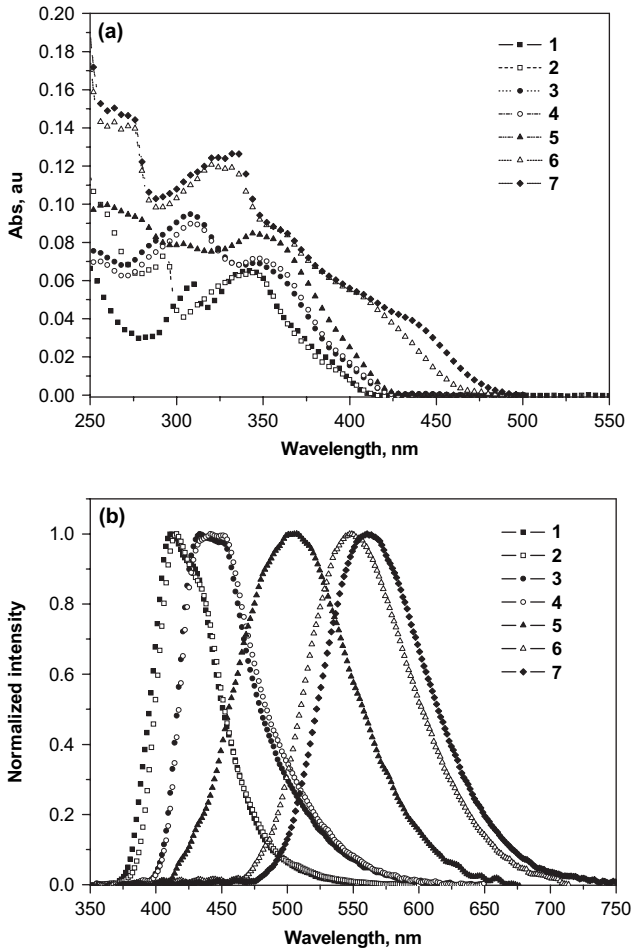

Figure 2. (a) Absorption and (b) emission spectra of compounds **1**–**7** in CH_2Cl_2. The excitation wavelength in emission spectra is 345 nm.

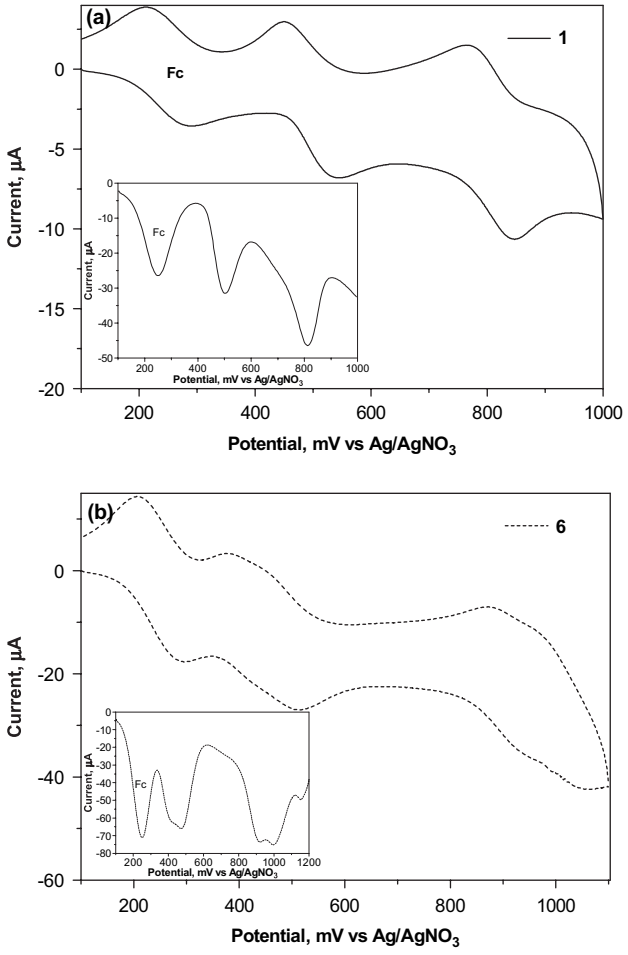

Figure 3. Cyclic voltammograms of (a) **1** and (b) **6** recorded in CH_2Cl_2 (scan rate 100 mV/s). Inset: different pulse voltammograms in the oxidization region.

peripheral amines in these compounds is in contrast to the 3,6-diarylamine substituted carbazoles (*carb*) we reported earlier, and can be attributed to the longer distance between the two peripheral amines.[4] In *carb* compounds, the two peripheral amines are electronically communicated and two one-electron oxidation waves are observed. The first oxidation potential of the carb compounds is, therefore, more cathodic than that of the compounds in this study.

Double-layer EL devices using compounds **1**, **2**, and **3** as the hole-transporting (HTL) as well as emitting layer and TPBI (1,3,5-tris(*N*-phenylbenzimidazol-2-yl)benzene) (device **I**) or Alq_3 (tris(8-quinolinolato)aluminum) (device **II**) as electron-transporting layer (ETL) were fabricated with the structure: ITO/**Cpd** (40 nm)/TPBI or Alq_3 (40 nm)/LiF (1 nm)/Al (200 nm) (**Cpd**=**1**, **2**, or **3**). Relative energy alignment of the constituents is shown in Figure 4 and the device performance parameters are collected in Table 2. Device **I** containing compounds **1** and **2** emitted blue light characteristic of the carbazole dimer derivatives while the device containing **3** emitted greenish blue light, which possibly resulted from the exciplex generated at the interface between the compound and TPBI layer. The electroluminescent (EL) spectra were shown in Figure 5. Such an outcome may be due to the higher hole mobility of **3** than **1** or **2**, which facilitated the carrier recombination to occur between the two layers.[19] In order to verify this argument, device **III** of the

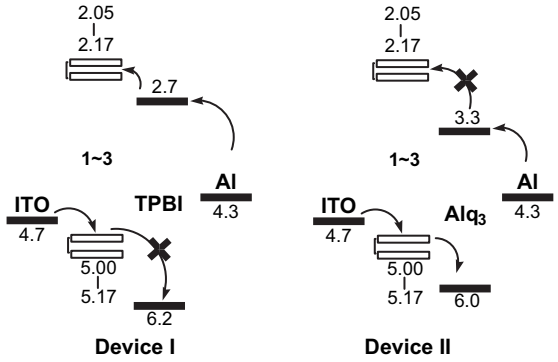

Figure 4. Energy alignment of the constituents in device **I** and device **II**.

Table 2. Electroluminescence data for the devices **I** and **II**[a]

	1 TPBI/Alq_3	**2** TPBI/Alq_3	**3** TPBI/Alq_3
V_{on}, V	3.0/2.5	4.0/3.5	3.0/2.5
L_{max}, cd/m^2	8703/36913	5533/28526	10817/24494
λ_{em}, nm	454/522	454/520	484/526
CIE (*x*, *y*)	0.17, 0.19/0.30, 0.56	0.16, 0.15/0.30, 0.54	0.20, 0.31/0.32, 0.56
fwhm, nm	82/94	74/96	92/98
$\eta_{ext,max}$, %	2.25/1.47	2.41/1.56	1.31/1.03
$\eta_{p,max}$, lm/W	1.92/2.91	1.95/3.05	2.34/1.75
$\eta_{c,max}$, cd/A	3.26/4.74	2.93/4.96	2.77/3.31
L, cd/m^2 (*)	3100/4347	2334/4776	2549/3306
η_{ext}, % (*)	2.14/1.47	1.93/1.51	1.21/1.02
η_p, lm/W (*)	1.31/1.88	0.88/1.79	1.14/1.35
η_c, cd/A (*)	3.10/4.74	2.35/4.78	2.56/3.31

[a] The measured values are given in the order of devices **I** and device **II**. L_{max}, maximum luminance; L, luminance; V_{on}, turn-on voltage; V, voltage; $\eta_{ext,max}$, maximum external quantum efficiency; $\eta_{p,max}$, maximum power efficiency; $\eta_{c,max}$, maximum current efficiency; η_{ext}, external quantum efficiency; η_p, power efficiency; η_c, current efficiency; fwhm, full width at half maximum; *, at a current density of 100 mA/cm^2. V_{on} was obtained from the *x*-intercept of log (luminance) versus applied voltage plot.

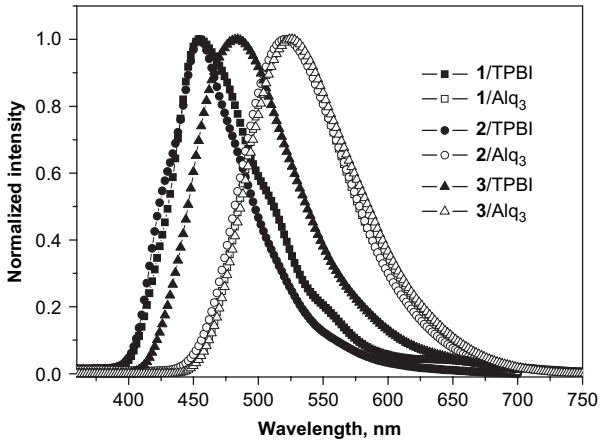

Figure 5. EL curves for device **I** and device **II** containing **1**, **2**, and **3**.

configuration ITO/**3** (60 nm)/TPBI (20 nm)/LiF (1 nm)/Al (200 nm) was fabricated. The thicker HTL and thinner ETL led to better balance of electrons and holes in the device **III**. Consequently, the EL spectrum of the device **III** matched with the film spectrum of **3** at an operating voltage of 6 V (Fig. 6). As the applied voltage increased, more holes reached the interface of HTL and ETL and more exciplexes were generated (Inset of Fig. 6). At a voltage of 12 V, the EL spectrum was nearly superimposable with that of the device **I** operated at 6 V. Such an explanation was further supported by the similar emission spectrum between device **I** and a mixed film of TPBI and **3**, where the exciplex of them should surely generate. Device **II** containing **1**, **2**, or **3** emitted green light from Alq_3. We believe that the HOMO energy gap (ΔE=1.03−1.20 eV) between HTL and ETL in the device **I** is sufficiently large to effectively block the injection of holes from the **Cpd** layer to the TPBI layer. In contrast, the smaller HOMO energy gap (ΔE=1.00–0.83 eV) between HTL and ETL allowed easier injection of holes from **Cpd** into the Alq_3 layer in the device **II**. This result is consistent with our previous studies in arylamine-containing carbazole derivatives.[4]

The current–voltage (I–V), luminance–current (L–I), and current efficiency–current density curves of devices **I** and **II** were shown in Figures 7–9. The relative low turn-on

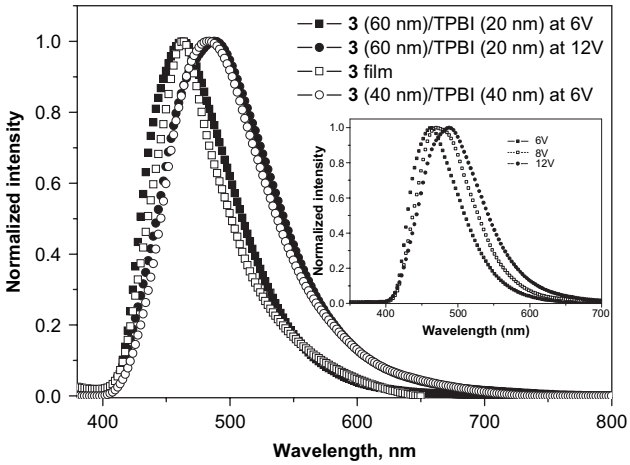

Figure 6. Comparison of EL and film PL curves for **3**. Inset: EL spectra of the device ITO/**3** (60 nm)/TPBI (20 nm)/LiF/Al at 6, 8, and 12 V.

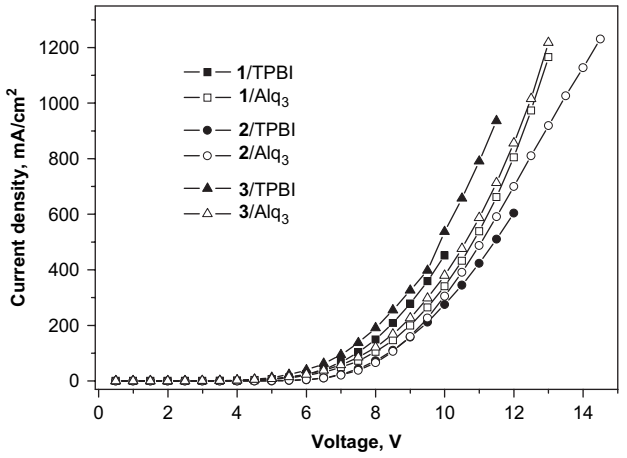

Figure 7. I–V curves for device **I** and device **II** containing compounds **1**, **2**, and **3**.

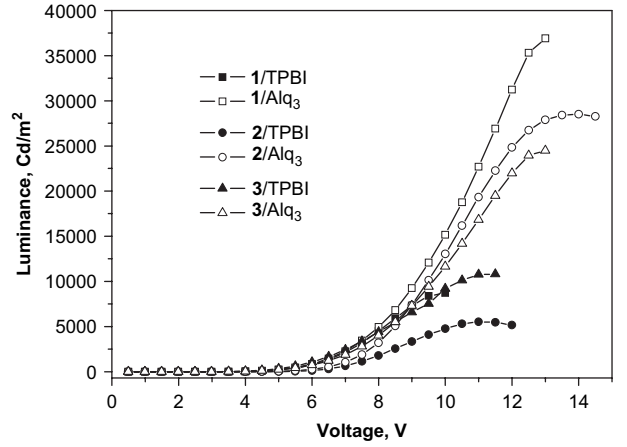

Figure 8. L–V curves for device **I** and device **II** containing **1**, **2**, and **3**.

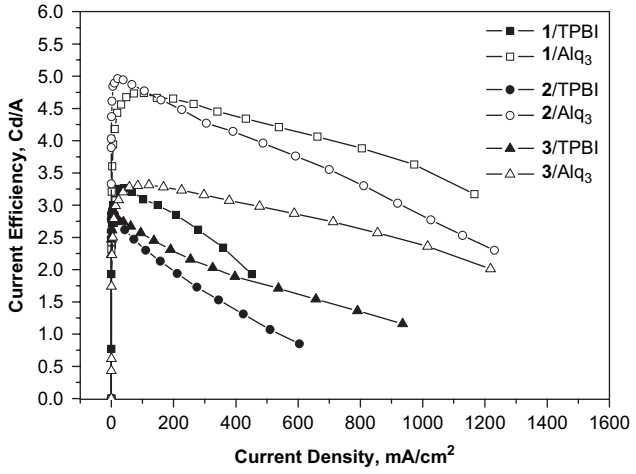

Figure 9. Current efficiency–current density curves for device **I** and device **II** containing **1**, **2**, and **3**.

and operating voltages in all devices **I** and **II** makes them promising for better performances. For blue emitting device **I**, the Commission International de l'Éclairage (CIE) coordinates (x, y) of **1**, **2**, and **3** are located at (0.17, 0.19), (0.16, 0.15), and (0.20, 0.31), respectively. They also exhibit good performance at operating voltage (e.g., L=2334–3100 cd/m^2; η_{ext}=1.2–2.1%; η_p=0.9–1.3 lm/W; η_c=2.4–3.1 cd/A at a current density of 100 mA/cm^2). For green-emitting device **II**, the CIE coordinates (x, y) are almost superimposable ((0.30, 0.56), (0.30, 0.54), and (0.32, 0.56) for **1**, **2** and **3**, respectively). The performance without optimization appear to be approximately equal (e.g., L_{max}= 24494–36913 cd/m^2; $\eta_{ext,\ max}$=1.0–1.6%; $\eta_{p,\ max}$=1.8–3.1 lm/W; $\eta_{c,\ max}$=3.3–5.0 cd/A) compared with the standard device of the structure ITO/α-NPD (40 nm)/Alq_3 (40 nm)/ LiF (1 nm)/Al (150 nm) referred in previous literature.[20]

3. Conclusions

To summarize, we have prepared a series of stilbene like carbazolyl derivatives by incorporating diarylamines at the peripheries of a carbazole dimer unit via McMurry C–C coupling reaction followed by palladium(0)-catalyzed C–N bond formation. The arylamine substituents significantly enhance the thermal stability of the carbazole dimer core. By altering the peripheral amines, the emitted color of these materials can be tuned from blue to yellow with moderate to good quantum yields. Double-layer devices using **1**–**3** as hole-transporting and emitting layer were fabricated. These devices exhibit very promising performance in blue or green region when TPBI and Alq_3 were selected as electron-transporting layers.

4. Experimental

4.1. General

Unless otherwise specified, all the reactions were carried out under nitrogen atmosphere using standard Schlenk techniques. Solvents were dried by standard procedures. All column chromatography was performed with the use of silica gel (230–400 mesh, Macherey-Nagel GmbH & Co.) as stationary phase. The ^{1}H NMR spectra were recorded on a Bruker AMX400 spectrometer. Electronic absorption spectra were measured in toluene, dichloromethane, and acetonitrile using a Cary 50 Probe UV–vis spectrophotometer. Emission spectra were recorded by a Jasco FP-6500 fluorescence spectrometer. Emission quantum yields were measured in various organic solvents by standard methods with reference to Coumarin 1 in acetonitrile. Cyclic voltammetry experiments were performed with a CHI-621B electrochemical analyzer. All measurements were carried out at room temperature with a conventional three-electrode configuration consisting of platinum working and auxiliary electrodes and a nonaqueous $Ag/AgNO_3$ reference electrode. The $E_{1/2}$ values were determined as $1/2(E_p^a+E_p^c)$, where E_p^a and E_p^c were the anodic and cathodic peak potentials, respectively. The solvent in all experiments was CH_2Cl_2 and the supporting electrolyte was 0.1 M tetrabutylammonium perchlorate. DSC measurements were carried out using a Perkin–Elmer 7 series thermal analyzer at a heating rate of 10 °C/min. TGA measurements were performed on a Perkin–Elmer TGA7 thermal analyzer. FAB-mass spectra were collected on a JMS-700 double focusing mass spectrometer (JEOL, Tokyo, Japan) with a resolution of 8000 (5% valley definition). For FAB-mass spectra, the source accelerating

voltage was operated at 10 kV with a Xe gun, using 3-nitrobenzyl alcohol as the matrix. Elementary analyses were performed on a Perkin–Elmer 2400 CHN analyzer.

4.2. Synthesis

6-Bromo-9-ethyl-9*H*-carbazole-3-carbaldehyde (**9**) was synthesized by following literature procedures.[21] (*E*)-1,2-Bis(9-ethyl-9*H*-carbazol-3-yl)ethene (**1**) and (*E*)-1,2-bis(6-bromo-9-ethyl-9*H*-carbazol-3-yl)ethene (**10**) were synthesized by similar procedure. Only the preparation of **10** will be described in detail.

4.2.1. (*E*)-1,2-Bis(6-bromo-9-ethyl-9*H*-carbazol-3-yl)-ethene (10). A mixture of 6-bromo-9-ethyl-9*H*-carbazole-3-carbaldehyde (6.04 g, 20 mmol) and zinc powder (3.92 g, 60 mmol) in a 250 mL two-neck flask was added dry THF. Titanium(IV) chloride (3.29 mL, 30 mmol) was added dropwise to the flask immersed in an ice bath. The ice bath was removed after addition was complete, and the reaction mixture was refluxed under nitrogen for 4 h. After being cooled, the solution was added to ice water and extracted with dichloromethane. The organic layer was collected, washed with brine, and dried over anhydrous $MgSO_4$. After filtration and removal of the solvent, the crude product was further recrystallized from CH_2Cl_2/hexane to give **1** as a pale yellow solid. Yield: 85%. ^{1}H NMR (δ, $CDCl_3$): 1.43 (t, J=3.6 Hz, 6H), 4.34 (q, J=7.2 Hz, 4H), 7.26 (d, J=8.6 Hz, 2H), 7.31 (s, 2H), 7.38 (d, J=8.5 Hz, 2H), 7.53 (dd, J=8.6, 1.9 Hz, 2H), 7.72 (dd, J=8.5, 1.6 Hz, 2H), 8.18 (d, J=1.2 Hz, 2H), 8.23 (d, J=1.9 Hz, 2H). FABMS (*m*/*z*): 571.9 (M^+).

4.2.2. (*E*)-1,2-Bis(9-ethyl-9*H*-carbazol-3-yl)ethene (1). White solids. Yield: 90%. ^{1}H NMR (δ, $CDCl_3$): 1.44 (t, J=3.6 Hz, 6H), 4.37 (q, J=7.2 Hz, 4H), 7.23 (d, J=8.6 Hz, 2H), 7.35 (s, 2H), 7.39 (d, J=8.5 Hz, 4H), 7.44 (t, J=7.4 Hz, 2H), 7.71 (dd, J=8.5, 1.6 Hz, 2H), 8.13 (d, J=7.6 Hz, 2H), 8.26 (d, J=1.9 Hz, 2H). ^{13}C NMR ($CDCl_3$): 140.3, 139.4, 129.2, 127.0, 125.7, 124.3, 123.3, 123.0, 120.5, 118.9, 118.3, 108.6, 108.5, 37.6, 13.9. FABMS (*m*/*z*): 414.1 (M^+). Anal. Calcd for $C_{30}H_{26}N_2$: C, 86.92; H, 6.32; N, 6.76. Found: C, 86.50; H, 6.28; N, 6.37.

(*E*)-1,2-Bis(9-ethyl-3,9′-bi(9*H*-carbazol)-6-yl)ethene (**2**), (*E*)-6,6′-(ethene-1,2-diyl)bis(9-ethyl-*N*,*N*-diphenyl-9*H*-carbazol-3-amine) (**3**), (*E*)-6,6′-(ethene-1,2-diyl)bis(9-ethyl-*N*-phenyl-*N*-*m*-tolyl-9*H*-carbazol-3-amine) (**4**), (*E*)-6,6′-(ethene-1,2-diyl)bis(9-ethyl-*N*-(naphthalen-1-yl)-*N*-phenyl-9*H*-carbazol-3-amine) (**5**), (*E*)-6,6′-(ethene-1,2-diyl)bis(9-ethyl-*N*-phenyl-*N*-(pyren-1-yl)-9*H*-carbazol-3-amine) (**6**), and (*E*)-6,6′-(ethene-1,2-diyl)bis(9-ethyl-*N*-(4-methoxyphenyl)-*N*-(pyren-1-yl)-9*H*-carbazol-3-amine) (**7**) were synthesized by a similar procedure as described for **2**.

4.2.3. (*E*)-1,2-Bis(9-ethyl-3,9′-bi(9*H*-carbazol)-6-yl)-ethene (2). The mixture of carbazole (0.37 g, 2.2 mmol), compound **1** (0.57 g, 1.0 mmol), sodium *tert*-butoxide (0.29 g, 3.0 mmol), $Pd(OAc)_2$ (9.0 mg, 0.040 mmol), tri(*tert*-butyl)phosphine (11 mg, 0.040 mmol), and dry toluene (20 mL) were refluxed under nitrogen for 16 h. After cooling, it was quenched with water and extracted with dichloromethane. The combined organic layer was washed with brine solution and dried over anhydrous $MgSO_4$. After filtration and removal of the solvent, the crude product was further purified by column chromatography on silica gel using dichloromethane/hexane=1/4 as the eluant to yield **2** as a pale yellow solid. Yield: 75%. ^{1}H NMR (δ, $CDCl_3$): 1.52 (t, J=3.6 Hz, 6H), 4.45 (q, J=7.2 Hz, 4H), 7.25–7.29 (m, 4H), 7.31 (s, 2H), 7.36–7.38 (m, 8H), 7.45 (d, J=9.6 Hz, 2H), 7.58 (dd, J=9.5, 8.6 Hz, 4H), 7.74 (dd, J=8.5, 1.6 Hz, 2H), 8.16 (d, J=7.7 Hz, 4H), 8.21 (s, 2H), 8.25 (s, 2H). ^{13}C NMR ($CDCl_3$): 141.9, 140.1, 139.4, 129.6, 129.0, 127.1, 125.8, 125.3, 125.0, 123.9, 123.1, 123.0, 120.3, 120.2, 119.7, 119.5, 119.4, 118.5, 110.5, 109.8, 109.5, 109.0, 38.0, 14.0. FABMS (*m*/*z*): 744.2 (M^+). Anal. Calcd for $C_{54}H_{40}N_4$: C, 87.07; H, 5.41; N, 7.52. Found: C, 86.80; H, 5.29; N, 7.47.

4.2.4. (*E*)-6,6′-(Ethene-1,2-diyl)bis(9-ethyl-*N*,*N*-diphenyl-9*H*-carbazol-3-amine) (3). Pale yellow solid. Yield: 79%. ^{1}H NMR (δ, $CDCl_3$): 1.47 (t, J=3.6 Hz, 6H), 4.35 (q, J=7.2 Hz, 4H), 6.95 (t, J=6.8 Hz, 4H), 7.12 (d, J=7.9 Hz, 8H), 7.22 (d, J=7.9 Hz, 8H), 7.25 (s, 2H), 7.29–7.38 (m, 6H), 7.65 (dd, J=8.5, 1.6 Hz, 2H), 7.91 (s, 2H), 8.11 (s, 2H). ^{13}C NMR ($CDCl_3$): 148.7, 139.9, 139.6, 137.6, 129.2, 129.0, 126.8, 125.5, 124.6, 123.9, 123.0, 122.7, 121.5, 118.9, 118.3, 109.4, 108.7, 37.8, 14.0. FABMS (*m*/*z*): 748.5 (M^+). Anal. Calcd for $C_{54}H_{44}N_4$: C, 86.60; H, 5.92; N, 7.48. Found: C, 86.20; H, 6.24; N, 7.30.

4.2.5. (*E*)-6,6′-(Ethene-1,2-diyl)bis(9-ethyl-*N*-phenyl-*N*-*m*-tolyl-9*H*-carbazol-3-amine) (4). Pale yellow solid. Yield: 80%. ^{1}H NMR (δ, $CDCl_3$): 1.45 (t, J=3.6 Hz, 6H), 2.23 (s, 6H), 4.33 (q, J=7.2 Hz, 4H), 6.77 (d, J=8.6 Hz, 2H), 6.88–6.93 (m, 6H), 7.07–7.13 (m, 6H), 7.19 (d, J=7.9 Hz, 4H), 7.22 (s, 2H), 7.26–7.36 (m, 6H), 7.63 (dd, J=8.5, 1.6 Hz, 2H), 7.89 (s, 2H), 8.10 (s, 2H). ^{13}C NMR ($CDCl_3$): 148.5, 139.1, 137.1, 131.5, 128.9, 128.7, 125.8, 123.9, 123.2, 122.5, 122.2, 120.4, 119.8, 119.7, 109.2, 108.5, 37.7, 21.5, 14.0. FABMS (*m*/*z*): 776.4 (M^+). Anal. Calcd for $C_{56}H_{48}N_4$: C, 86.56; H, 6.23; N, 7.21. Found: C, 86.48; H, 6.31; N, 6.88.

4.2.6. (*E*)-6,6′-(Ethene-1,2-diyl)bis(9-ethyl-*N*-(naphthalen-1-yl)-*N*-phenyl-9*H*-carbazol-3-amine) (5). Yellow solid. Yield: 70%. ^{1}H NMR (δ, $CDCl_3$): 1.52 (t, J=3.6 Hz, 6H), 4.45 (q, J=7.2 Hz, 4H), 6.84–6.91 (m, 6H), 7.15 (t, J=7.9 Hz, 4H), 7.19 (s, 2H), 7.26–7.37 (m, 10H), 7.42–7.50 (m, 4H), 7.60 (dd, J=8.5, 1.6 Hz, 2H), 7.73 (d, J=8.2 Hz, 2H), 7.88 (d, J=8.2 Hz, 2H), 7.91 (d, J=1.9 Hz, 2H), 8.04 (d, J=1.2 Hz, 2H), 8.08 (d, J=8.6 Hz, 2H). ^{13}C NMR ($CDCl_3$): 150.1, 144.5, 140.7, 139.9, 137.1, 135.3, 131.1, 129.0, 128.9, 128.3, 126.8, 126.4, 126.2, 126.0, 125.8, 124.6, 124.4, 123.9, 123.6, 123.0, 119.9, 119.6, 118.3, 116.8, 115.2, 109.1, 108.6, 37.7, 14.0. FABMS (*m*/*z*): 848.4 (M^+). Anal. Calcd for $C_{62}H_{48}N_4$: C, 87.70; H, 5.70; N, 6.60. Found: C, 88.09; H, 5.95; N, 6.37.

4.2.7. (*E*)-6,6′-(Ethene-1,2-diyl)bis(9-ethyl-*N*-phenyl-*N*-(pyren-1-yl)-9*H*-carbazol-3-amine) (6). Yellow solid. Yield: 77%. ^{1}H NMR (δ, $CDCl_3$): 1.42 (t, J=3.6 Hz, 6H), 4.28 (q, J=7.2 Hz, 4H), 6.87 (t, J=7.3 Hz, 2H), 6.95 (d, J=7.7 Hz, 4H), 7.14 (s, 2H), 7.17 (d, J=7.7 Hz, 4H), 7.26–7.29 (m, 4H), 7.34 (dd, J=8.7, 2.1 Hz, 2H), 7.55 (dd, J=8.4, 1.3 Hz, 2H), 7.86 (d, J=8.2 Hz, 2H), 7.90–7.96 (m, 8H), 8.03 (s, 4H), 8.08 (d, J=7.5 Hz, 2H), 8.12–8.16

ARTICLE IN PRESS

(m, 4H), 8.26 (d, J=9.2 Hz, 2H). ^{13}C NMR ($CDCl_3$): 150.2, 141.9, 140.9, 139.9, 137.0, 131.3, 131.1, 129.1, 129.0, 127.6, 127.3, 126.8, 126.1, 126.0, 125.0, 124.9, 123.7, 122.9, 120.1, 119.9, 118.2, 116.9, 109.2, 108.6, 37.7, 13.9. FABMS (m/z): 996.3 (M^+). Anal. Calcd for $C_{74}H_{52}N_4$: C, 89.13; H, 5.26; N, 5.62. Found: C, 88.80; H, 5.48; N, 5.52.

4.2.8. (*E*)-6,6′-(Ethene-1,2-diyl)bis(9-ethyl-*N*-(4-methoxy-phenyl)-*N*-(pyren-1-yl)-9*H*-carbazol-3-amine) (7). Yellow solid. Yield: 65%. ^{1}H NMR (δ, $CDCl_3$): 1.38 (t, J=3.6 Hz, 6H), 3.75 (s, 6H), 4.26 (q, J=7.2 Hz, 4H), 6.74 (d, J=7.7 Hz, 4H), 6.99 (d, J=7.7 Hz, 4H), 7.12 (s, 2H), 7.15–7.26 (m, 6H), 7.54 (dd, J=8.4, 1.3 Hz, 2H), 7.80 (d, J=8.2 Hz, 2H), 7.83–7.96 (m, 8H), 8.03 (s, 4H), 8.05–8.13 (m, 6H), 8.26 (d, J=9.2 Hz, 2H). ^{13}C NMR ($CDCl_3$): 136.5, 131.4, 131.2, 128.9, 128.6, 127.3, 126.6, 126.5, 126.1, 125.9, 125.0, 124.8, 124.7, 123.9, 123.2, 123.0, 122.8, 120.5, 118.2, 115.3, 114.5, 109.1, 108.5, 55.5, 37.7, 14.0. FABMS (m/z): 1056.2 (M^+). Anal. Calcd for $C_{76}H_{56}N_4O_2$: C, 86.34; H, 5.34; N, 5.30. Found: C, 85.91; H, 5.65; N, 5.46.

4.3. OLEDs fabrication and measurements

Electron-transporting materials TPBI and Alq_3 were synthesized according to literature procedures and were sublimed twice prior to use. Pre-patterned ITO substrates with an effective individual device area of 3.14 mm^2 were cleaned as described in a previous report.[22] Double-layer EL devices using carbazole derivatives as the hole-transport layer and TPBI or Alq_3 as the electron-transport layer were fabricated. For comparison, a typical device using NPB (1,4-bis(1-naphthylphenylamino)biphenyl) as the hole-transporting layer was also fabricated. All devices were prepared by vacuum deposition of 40 nm of the hole-transporting layer, followed by 40 nm of TPBI or Alq_3, and then 1 nm of LiF and 200 nm of Al were deposited as the cathode. I–V curve was measured on a Keithley 2400 source meter in an ambient environment. Light intensity was measured with a Newport 1835 optical meter.

Acknowledgements

We are thankful to Academia Sinica, National Taiwan Normal University, and National Science Council for financial support.

References and notes

1. Tang, C. W.; VanSlyke, S. A. *Appl. Phys. Lett.* **1987**, *51*, 913.
2. Lin, X. Q.; Chen, B. J.; Zhang, X. H.; Lee, C. S.; Kwong, H. L.; Lee, S. T. *Chem. Mater.* **2001**, *13*, 456.
3. Yang, Y.; Pei, Q.; Heeger, A. J. *J. Appl. Phys.* **1996**, *79*, 934.
4. Justin Thomas, K. R.; Lin, J. T.; Tao, Y.-T.; Ko, C.-W. *J. Am. Chem. Soc.* **2001**, *123*, 9404.
5. (a) McClenaghan, N. D.; Passalacqua, R.; Loiseau, F.; Campagna, S.; Verheyde, B.; Hameurlaine, A.; Dehaen, W. *J. Am. Chem. Soc.* **2003**, *125*, 5356; (b) Kimoto, A.; Cho, J.-S.; Higuchi, M.; Yamamoto, K. *Macromolecules* **2004**, *37*, 5531.
6. (a) Qiu, S.; Liu, L. L.; Wang, B. L.; Shen, F. Z.; Zhang, W.; Li, M.; Ma, Y. G. *Macromolecules* **2005**, *38*, 6782; (b) Jiang, J.; Jiang, C. Y.; Yang, W.; Zhen, H. Y.; Huang, F.; Cao, Y. *Macromolecules* **2005**, *38*, 4072.
7. (a) Brunner, K.; Dijken, A. V.; Börner, H.; Bastiaansen, J. J. A. M.; Kiggen, N. M. M.; Langeveld, B. M. W. *J. Am. Chem. Soc.* **2004**, *126*, 6035; (b) Wong, K.-T.; Chen, Y.-M.; Lin, Y.-T.; Su, H.-C.; Wu, C.-C. *Org. Lett.* **2005**, *7*, 5361.
8. Ko, C.-W.; Tao, Y.-T.; Lin, J. T.; Justin Thomas, K. R. *Chem. Mater.* **2002**, *14*, 357.
9. Li, J.; Liu, D.; Li, Y. Q.; Lee, C.-S.; Kwong, H.-L.; Lee, S. *Chem. Mater.* **2005**, *17*, 1208.
10. (a) Morin, J.-F.; Leclerc, M. *Macromolecules* **2002**, *35*, 8413; (b) Justin Thomas, K. R.; Lin, J. T.; Tao, Y.-T.; Chuen, C.-H. *Chem. Mater.* **2002**, *14*, 3852.
11. Grigalevicius, S. *Synth. Met.* **2006**, *156*, 1.
12. (a) Ko, C.-W.; Tao, Y.-T. *Chem. Mater.* **2001**, *13*, 2441; (b) Huang, L.; Tian, H.; Li, F.-Y.; Gao, D.-Q.; Huang, Y.-Y.; Huang, C.-H. *J. Lumin.* **2002**, *97*, 55; (c) Lee, M.-T.; Liao, C.-H.; Tsai, C.-H.; Chen, C. H. *Adv. Mater.* **2005**, *17*, 2493.
13. Sonntag, M.; Strohriegl, P. *Chem. Mater.* **2004**, *16*, 4736.
14. (a) Shi, J.; Tang, C. W.; Chen, C. H. U.S. Patent 5,645,948, 1997; (b) Sonsale, A. Y.; Gopinathan, S.; Gopinathan, C. *Indian J. Chem.* **1976**, *14*, 408.
15. Chen, C. H.; Shi, J.; Tang, C. W. *Coord. Chem. Rev.* **1998**, *171*, 161.
16. Vilsmeier, A.; Haack, A. *Chem. Ber.* **1927**, *60*, 119.
17. Hartwig, J. F.; Kawatsura, M.; Hauck, S. I.; Shaughnessy, K. H.; Alcazar-Roman, L. M. *J. Org. Chem.* **1999**, *64*, 5575.
18. Kim, Y. E.; Kwon, Y. S.; Lee, K. S.; Park, J. W. *Mol. Cryst. Liq. Cryst.* **2004**, *424*, 153.
19. (a) Blazys, G.; Grigalevicius, S.; Grigalevicius, J. V.; Gaidelis, V.; Jankauskas, V.; Kampars, V. *J. Photochem. Photobiol. A: Chem.* **2005**, *174*, 1; (b) Grigalevicius, S.; Getautis, V.; Grigalevicius, J. V.; Gaidelis, V.; Jankauskas, V.; Montrimas, E. *Mater. Chem. Phys.* **2001**, *72*, 395.
20. Huang, T.-H.; Whang, W.-T.; Shen, J. Y.; Lin, J. T.; Zheng, H. G. *J. Mater. Chem.* **2005**, *15*, 3233.
21. (a) Moon, H.; Hwang, J.; Kim, N.; Park, S. Y. *Macromolecules* **2000**, *33*, 5116; (b) Justin Thomas, K. R.; Velusamy, M.; Lin, J. T.; Tao, Y.-T.; Chuen, C.-H. *Adv. Funct. Mater.* **2004**, *14*, 387.
22. Wu, I.-Y.; Lin, J. T.; Tao, Y.-T.; Balasubramaniam, E.; Su, Y.-Z.; Ko, C.-W. *Chem. Mater.* **2001**, *13*, 2626.